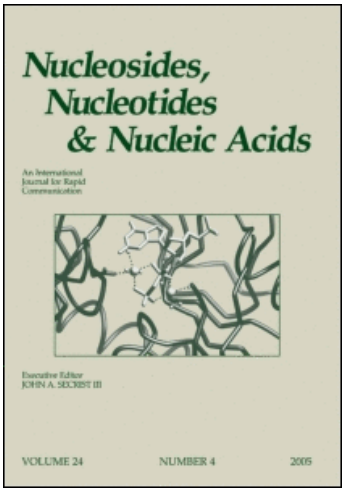

Nucleosides, Nucleotides and Nucleic Acids
Publication details, including instructions for authors and subscription information:
http://www.informaworld.com/smpp/title~content=t713597286

Hydrodynamic and Spectroscopic Studies of Substrate Binding to Human Recombinant Deoxycytidine Kinase

Rajam S. Mani[ab]; Elena V. Usova[c]; Staffan Eriksson[c]; Carol E. Cass[ab]
[a] Department of Oncology, Cross Cancer Institute, University of Alberta, Alberta, Edmonton, Canada [b] Department of Oncology, Cross Cancer Institute, Edmonton, AB, Canada [c] Department of Veterinary Medical Chemistry, The Biomedical Centre, Swedish University of Agricultural Sciences, Uppsala, Sweden

Online publication date: 15 April 2003

To cite this Article Mani, Rajam S. , Usova, Elena V. , Eriksson, Staffan and Cass, Carol E.(2003) 'Hydrodynamic and Spectroscopic Studies of Substrate Binding to Human Recombinant Deoxycytidine Kinase', Nucleosides, Nucleotides and Nucleic Acids, 22: 2, 175 — 192
To link to this Article: DOI: 10.1081/NCN-120019513
URL: http://dx.doi.org/10.1081/NCN-120019513

NUCLEOSIDES, NUCLEOTIDES & NUCLEIC ACIDS
Vol. 22, No. 2, pp. 175–192, 2003

Hydrodynamic and Spectroscopic Studies of Substrate Binding to Human Recombinant Deoxycytidine Kinase

Rajam S. Mani,[1,*] Elena V. Usova,[2] Staffan Eriksson,[2] and Carol E. Cass[1,*]

[1]Department of Oncology, Cross Cancer Institute, University of Alberta, Edmonton, Alberta, Canada
[2]Department of Veterinary Medical Chemistry, The Biomedical Centre, Swedish University of Agricultural Sciences, Uppsala, Sweden

ABSTRACT

Deoxycytidine kinase (dCK), a cytosolic enzyme with broad substrate specificity, plays a key role in the activation of therapeutic nucleoside analogues by their 5′-phosphorylation. The structure of human dCK is still not known and the current work was undertaken to determine its oligomeric and secondary structure. Biophysical studies were conducted with purified recombinant human dCK. The M_r determined by low-speed sedimentation equilibrium under nondenaturing conditions was 60,250 ± 1,000, indicating that dCK, which has a predicted M_r of 30,500, exists in solution as a dimer. Analysis of circular dichroism spectra revealed the presence of two negative dichroic bands located at 222 and 209 nm with ellipticity values of –11,900 ± 300 and −12,500 ± 300 deg·cm^2·dmol^{-1}, respectively, indicating the presence of approximately 40% α-helix and 50% β-structure. Circular Dichroism studies in the aromatic and far-ultraviolet range and UV difference spectroscopy indicated that binding of substrates to dCK

*Correspondence: Rajam S. Mani and Carol E. Cass, Department of Oncology, Cross Cancer Institute, 11560 University Avenue, Edmonton, AB, T6G 1Z2 Canada; Fax: 780-432-2445; E-mail: rajam.mani@cancerboard.ab.ca and carol.cass@cancerboard.ab.ca.

DOI: 10.1081/NCN-120019513
1525-7770 (Print); 1532-2335 (Online)

MARCEL DEKKER, INC.
270 Madison Avenue, New York, New York 10016

reduced its α-helical content and perturbed tryptophan and tyrosine. Steady-state fluorescence demonstrated that deoxycytidine (the phosphate acceptor) and ATP (the phosphate donor) bound to different sites on dCK and fluorescence quenching revealed bimodal binding of deoxycytidine and unimodal binding of ATP. Spectroscopic studies indicated that substrate binding induced conformational changes, with the result that dCK exhibited different affinities for various substrates. These results are consistent with a random bi-bi kinetic mechanism of phosphorylation of dCyd with either ATP or UTP.

Key Words: Deoxycytidine kinase; Gemcitabine; Circular dichroism; Fluorescence spectroscopy.

Abbreviations: dCK, deoxycytidine kinase; dCyd, 2′-deoxycytidine; cDNA, complementary DNA; His-tag, histidine affinity tag; dCTP, deoxycytidine triphosphate; CD, circular dichroism; DTT, dithiothreitol; PMSF, phenylmethanesulfonyl fluoride; SDS, sodium dodecyl sulfate; BSA, bovine serum albumin.

INTRODUCTION

Deoxycytidine kinase (dCK, EC 2:7.1.74) catalyses the 5′-phosphorylation of pyrimidine and purine deoxynucleosides using nucleoside triphosphates as phosphate donors. The produced deoxynucleoside monophosphates are then converted to deoxyribonucleoside triphosphates by the sequential action of nucleoside monophosphate kinases and nucleoside diphosphate kinase. dCK is important in nucleoside therapeutics since it phosphorylates many important anticancer and antiviral drugs.[1,2] This enzyme is abundant in proliferating cells and tissues but is absent or present in only low quantities in differentiated cells.[3,4] Regulation of the abundance of dCK involves both transcriptional and post-transcriptional processes.[5,6]

The cloning of the cDNA encoding dCK and characterization of recombinant dCK produced in *E. coli* has been described.[2,3] Although the structure of dCK has not yet been solved, the structure of human deoxyguanosine kinase, which has 40% identity in amino acid sequence to dCK, was recently determined by X-ray crystallography[7] and has been used to construct a 3.D model for dCK based on the amino-acid identity between the two proteins. According to this model, dCK is believed to exists as a dimer with an α/β architecture and the N-terminal phosphate binding loop at the center of the active site. Hydrophobic residues from helices α4 and α6 in the C-terminal part of the dCK monomer are predicted to be involved in subunit interactions, forming a four-helix bundle.

The phosphate donor specificity of dCK is broad. Most nucleoside triphosphates are accepted as substrates, the exception being dCTP, which acts as a feedback inhibitor. It has been suggested that UTP is the preferred phosphate donor in intact cells.[8–10] The K_m values for UTP and ATP are 1 and 54 μM, respectively, and the K_m values for nucleoside substrates are lower when UTP is used as the phosphate donor instead of ATP. The kinetic behavior of dCK is complex. It exhibits negative co-operativity for phosphate donors and acceptors, with Hill coefficients <1.[11–13] Steady-state substrate kinetic analyses with purified native and recombinant dCK have shown a random bi-bi pathway when ATP is used as the phosphate donor

Marcel Dekker, Inc.
270 Madison Avenue, New York, New York 10016

and an ordered reaction when UTP is used as the phosphate donor, with UTP binding before the nucleoside substrate.[11,13–15] Results obtained with fluorescence quenching experiments with native dCK[13] and stopped-flow fluorescence studies with recombinant dCK[15] suggest substrate-induced conformational changes. Thus, it is likely that dCK exists in different conformational states with different substrate-affinity profiles. The 3.D structural model recently proposed for dCK is not supported by the kinetic data in that the model, which places the nucleoside-binding site in the interior and the phosphate donor site on the exterior of the protein, predicts that the phosphate donor would bind after the nucleoside substrate.

To gain more insight into the changes that occur upon ligand binding to dCK and to resolve the discrepancy between the kinetic results and the structural model, a series of hydrodynamic and spectroscopic experiments were performed with recombinant dCK and different substrates, including dCyd, ATP, and UTP. We found that dCK was present as a dimer in solution. The results of our biophysical studies revealed that dCK underwent changes in its secondary and tertiary structures upon ligand binding that varied with the nature of the ligand.

MATERIALS AND METHODS

Enzyme Preparation and Purification

Recombinant human dCK was prepared and purified using the pET-9d bacterial vector system (Novagen, Madison) as described previously.[2] Expression of dCK was induced by addition of isopropyl thio-β-D-galactoside (IPTG) and growth was continued for 4 h at 37°C. Cells were harvested by centrifugation at 2400 g for 10 min at 4°C, resuspended and lysed by freeze-thawing and sonication 3×1 min on ice in 20 mM Tris-HCl (pH 7.9), 0.5 M NaCl, and 1 mM phenylmethanesulfonyl fluoride (PMSF). The lysate was then centrifuged at 26,000 g (2330 Ultraspin 55, LKB) for 1 h at 4°C and dCK was then purified from the lysate by metal chelation affinity chromatography. After unbound proteins were removed by washing, dCK was eluted with 0.5 M imidazole in 20 mM Tris-HCl (pH 7.9), 0.5 M NaCl, and 1 mM PMSF. The purity of the preparation was assessed using SDS-PAGE. The purified dCK was transferred from the elution buffer to 10 mM potassium-phosphate buffer (pH 7.3) using (PD-10) Sephadex® G-25 columns (Pharmacia Biotech). The histidine-tagged dCK contained a thrombin cleavage site fused to the N-termininus of dCK, and cleavage was performed using thrombin (Pharmacia) as described previously,[2] producing dCK with three additional amino acids: (glycine, serine, alanine) at the N-terminus. Cleavage was monitored by SDS-PAGE.

Gel Filtration Chromatography

Gel filtration chromatography was performed using fast protein liquid chromatography on a Superdex® 200 column with a Pharmacia Monitor UV-I I (Pharmacia Biotech) operating at 280 nm and a flow rate of 0.4 mL/min. The column was equilibrated and eluted with 10 mM potassium phosphate buffer (pH 7.3). Bovine serum albumin (BSA) (M_r 66,000) and carbonic anhydrase (M_r 29,000) were used as

Marcel Dekker, Inc.
270 Madison Avenue, New York, New York 10016

molecular weight markers. Protein fractions corresponding to 60 kD_a were collected and concentrated with the an Ultrafree®−15 (Millipore) centrifugal filter device.

Enzyme Assay

The enzyme activity was followed by a radiochemical assay procedure as described earlier[1] using 2′-[5-^{3}H]dCyd. Assays were performed in 50 mM Tris-HCl (pH 7.6), 100 mM KCl, 5 mM $MgCl_2$, 5 mM ATP, 2 mM dithiothreitol (DTT), 0.5 mg/mL BSA, 50 ng of pure dCK and 25 μM dCyd. The specific activity of the purified recombinant enzyme was approximately 60 nmol/min/mg.

Hydrodynamic Studies

Fringe counts were performed using a Beckman XLI analytical ultracentrifuge and double-sector capillary synthetic boundary cells as described.[16] Prior to ultracentrifugation, the dCK preparations were dialyzed for 48 h in 50 mM potassium phosphate (pH 7.4), 100 mM KCl, 5 mM $MgCl_2$ and 2 mM DTT. All hydrodynamic and spectroscopic studies were carried out using this potassium phosphate buffer system. The absorbance of dCK samples was measured using 1.0 cm path length cuvettes. dCK protein samples (150 μL) were loaded into one sector of the cell, and 400 μL of the dialysate was loaded into the other sector. Runs were performed at 8000 rpm, and scans were taken when fringes were resolved across the boundary region between the protein solution and solvent. The number of fringes produced across the boundary was measured and converted to concentration using an average increment of 3.31 fringes $mg^{-1}\,mL^{-1}$. From a plot of the number of fringes vs. optical density, a value of 20.7 was established as the extinction coefficient, $E^{1\%}_{1\text{ cm, }280\text{ nm,}}$ for dCK.

Sedimentation Velocity Measurements

Sedimentation velocity experiments were carried out at 20°C and 50,000 rpm using the XLI analytical ultracentrifuge and interference optics following the procedures described by Laue and Stafford[17] and as also outlined in the instruction manual (Spinco Business Center of Beckman Instruments, Inc., Palo Alto, CA). Four hundred μL of protein solution and 400 μL of dialysate were loaded into two sector CFE centerpiece cells containing sapphire windows. Runs were performed for 4 h, during which a minimum of 30 scans were taken. The sedimentation velocity data were analyzed according to Williams et al.[18] to determine the sedimentation coefficient, S. The intrinsic sedimentation coefficient, $S^0_{20,w}$, which represents the sedimentation coefficient corrected to water at 20°C, was then calculated from the observed S value as described by Laue et al.[19]

Sedimentation Equilibrium Studies

Sedimentation equilibrium experiments were carried out at 5°C using interference optics as described previously.[20] Protein samples (110 μL) were loaded into

Marcel Dekker, Inc.
270 Madison Avenue, New York, New York 10016

6-sector CFE cells, allowing two concentrations of dCK to be run simultaneously. Runs were performed at 16,000, and 20,000 rpm, and each speed was maintained until there was no significant difference in scans taken 2 h apart to ensure that equilibrium was achieved. The sedimentation equilibrium data were evaluated with the Nonlin analysis program using a nonlinear least-squares curve-fitting algorithm.[21] The program Sednterp (Sedimentation Interpretation Program, version 1.01) was employed to calculate the partial specific volume of dCK from its predicted amino acid composition using the method of Cohn and Edsall.[22]

UV Spectroscopy

UV absorption and UV difference spectra were recorded on a Perkin-Elmer Lambda 5 spectrophotometer over the wavelength range 320–250 nm with 1-cm path-length cells as described previously.[23] To generate a UV difference spectrum, solutions with 20 μM ligands (dCyd, ATP or UTP) and dCK (0.5 mg/mL) were added to the sample and reference cells with mixing only in the sample cell to allow interaction between dCK and the ligands to proceed. Corrections were made for dilutions before the spectra were analyzed.

Circular Dichroism Spectroscopy

Circular dichroism (CD) measurements were performed in a JASCO J-720 spectropolarimeter (Jasco, Easton, MD) calibrated with a 0.06% solution of ammonium d-camphor-10-sulfonate. The temperature in the sample chamber was maintained using a Lauda RM6 low–temperature circulator. Each sample was scanned 10 times, noise reduction was applied, and baseline buffer spectra in the absence and the presence of ligand were subtracted from the respective protein spectra in the absence and presence of ligand before calculating molar ellipticities. To obtain spectra in the far-UV region, the cell-path length was 0.02 cm, and the protein concentration was 0.5 mg/mL. To obtain the aromatic CD spectra, the cell-path length was 1 cm and the protein concentration was 1 mg/mL. The CD spectra were analyzed for secondary structure elements by the Contin ridge regression analysis program of Provencher and Glöckner.[24]

Fluorescence Studies

Steady-state fluorescence spectra were measured at room temperature on a Perkin-Elmer LS-50B spectrofluorometer (with 5-nm spectral resolution for excitation and emission) using 0.2–0.5 μM solutions of purified recombinant dCK. Protein fluorescence was excited at 285 nm, and fluorescence emission spectra were recorded in the 300–380-nm range; changes of fluorescence were usually monitored at the emission maximum (335 nm). In studying the effects of ligands on protein fluorescence intensity, additions to the dCK sample were made from ligand stock solutions, keeping the dilution below 5% and fluorescence intensity was normalized taking into

account the dilution factor. Background emission (<5%) was eliminated by subtracting the signal from buffer containing the appropriate quantity of ligand. The total absorption of the enzyme sample was kept below 0.1 at 285 nm.

RESULTS

Characterization of Recombinant Human dCK

The pET-9d vector and the *E. coli* strain BL21 (DE3) pLysS were used to produce recombinant human dCK with an N-terminal affinity tag of six histidines that enabled efficient purification as described earlier.[2] The histidine tag was removed by thrombin cleavage before biophysical studies were undertaken and the resulting protein differed from native human dCK by having three additional N-terminal amino acids: glycine, serine and alanine. The UV absorption spectrum of recombinant dCK exhibited an absorption maximum at 278 nm, characteristic of tyrosine residues, and a shoulder around 290 nm, characteristic of tryptophan residues. The 278/260 and 278/290 absorbance ratios were 1.47 and 1.51, respectively. Protein concentrations were determined using an extinction coefficient, $\epsilon^{1\%}_{278\,nm,}$ of 20.7, a value that was established by the refractometric method of Babul and Stellwagen.[16]

Sedimentation Velocity and Equilibrium Studies: Demonstration That dCK Exists as a Dimer

In the presence of the reducing agent DTT, the sedimentation profile of dCK exhibited a single symmetrical peak with no significant change in $s^0_{20,w}$ values (i.e., 4.30 S vs. 4.33 S in the absence and presence, respectively, of 20 μM ATP). This result demonstrated that dCK did not aggregate upon ATP binding. In the absence of DTT, aggregation was observed since higher $s^0_{20,w}$ values were obtained (i.e., 4.55 and 4.57, in the absence or presence of 20 μM ATP, respectively).

Sedimentation equilibrium studies were conducted to determine the oligomeric state of dCK (Fig. 1). In the presence of DTT, the sedimentation data fit well to a single species model with no evidence of any association and a calculated apparent M_r of 60,250, indicating that dCK was a dimer since its predicted sequence,[3] yields a M_r of 30,500 for a single polypeptide chain.[13] The M_r in the presence of 20 μM ATP was 61,000 (data not shown), indicating that dCK did not aggregate upon binding ATP, consistent with the sedimentation velocity results. In the absence of DTT, the weight average M_r values obtained without and with 20 μM ATP were 72,000, and 73,000, respectively, suggesting that 15 to 20% of the protein existed in a tetrameric form. The sedimentation coefficient ($s^0_{20,w}$ value), partial specific volume and molecular weight data allowed a hydrodynamic characterization of dCK using the Sednterp analysis.[20] dCK was found to have a Stokes radius, R_s, of 33.5 Å, and was globular in nature with an axial ratio of 2.73 (major axis/minor axis) for a prolate ellipsoid model, very much like BSA (M_r of 66,500), a globular protein with an axial ratio of 2.6.[20]

Marcel Dekker, Inc.
270 Madison Avenue, New York, New York 10016

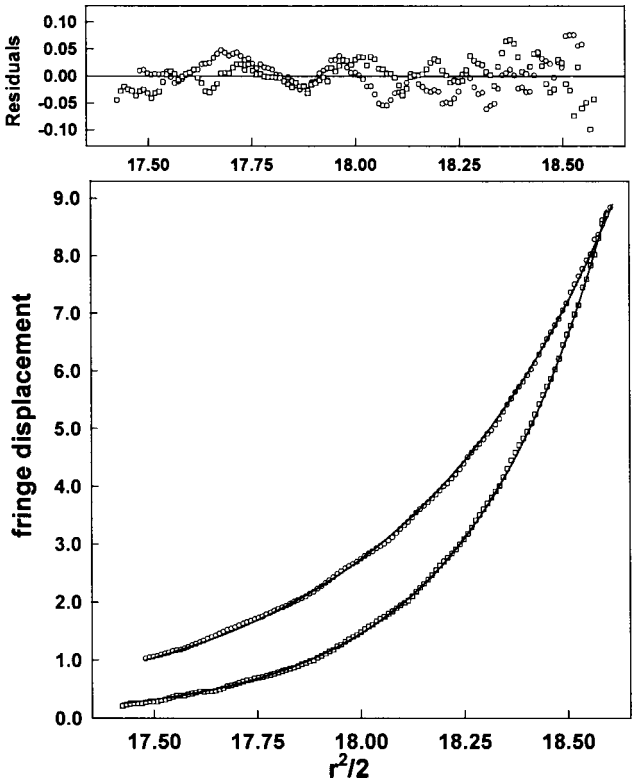

Figure 1. Sedimentation equilibrium profiles for human dCK obtained at 16,000 rpm (circles) and 20,000 rpm (squares) at 5°C in 50 mM potassium phosphate, 100 mM KCl, 5 mM $MgCl_2$, and 2 mM DTT for 48 h. The loading protein concentration was 1.2 mg/mL. Global nonlinear regression fitting of both data sets was performed for a single component system, and the solid lines denote the fitted curves. The residuals for each fit are shown in the upper panels above the absorbance vs. radial distribution profiles.

Secondary Structure of Human dCK: Effects of ATP and dCyd

Information regarding the secondary structure of dCK was obtained from CD studies. A typical far-UV CD spectrum in the presence of DTT is shown in Fig. 2. There were two large negative CD bands centered at 222 and 209 nm, and the molar ellipticities, $[\theta]_M$, at these two wavelengths were $-11{,}900 \pm 300$ and $-12{,}500 \pm 300$ deg.cm^2·dmol^{-1}, respectively. When the CD spectrum was analyzed for secondary structural elements by the Contin ridge regression analysis program,[24] dCK had ~40% α-helix and ~50% β-sheet–β-turn, with the remaining ~10% as random structure (Table 1).

It is evident from the results of Fig. 2 that addition of ATP induced a conformational change in dCK since the molar ellipticity values $[\theta]_M$, at 222 and 209 nm were reduced to $-10{,}700 \pm 300$ and $-11{,}250 \pm 300$ deg·cm^2·dmol^{-1}, respectively, with significant changes in secondary structure (Table 1). Binding of dCyd also altered

Marcel Dekker, Inc.
270 Madison Avenue, New York, New York 10016

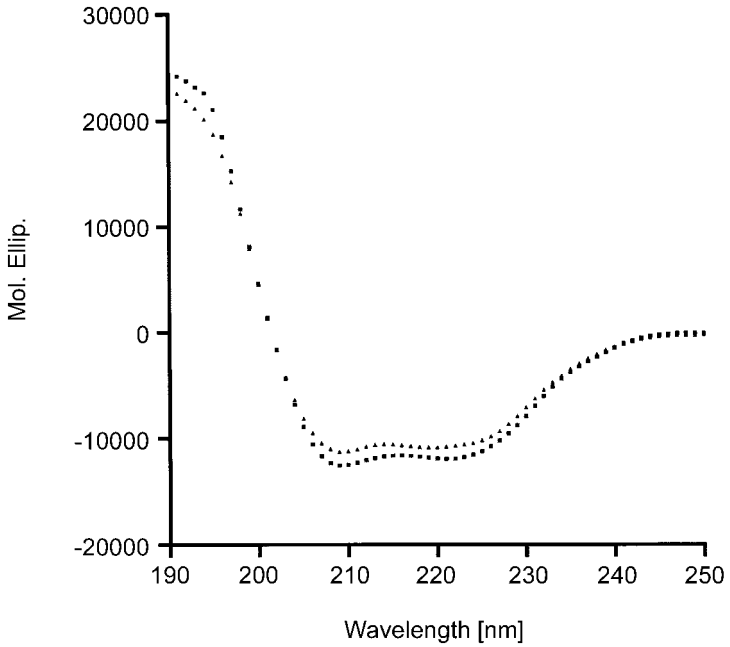

Figure 2. Far-UV CD spectra of human dCK were obtained as described in Materials and Methods in 50 mM potassium phosphate, pH 7.4, 100 mM KCl, 5 mM $MgCl_2$, and 2 mM DTT in the absence (■) and presence of 20 μM ATP (▲).

the CD spectrum (data not shown), reflecting conformational changes (Table 1) comprised of decreased α-helical and β-sheet content and increased random structure. Removal of Mg^{2+} ions by EDTA also altered the conformation of dCK, although to a lesser extent than was observed with addition of either ATP or dCyd.

Effects of UTP and Gemcitabine on Near-UV CD Spectra of Human dCK

Near-UV (250–320 nm) CD spectroscopy provides information on the environment of aromatic residues in folded proteins. The aromatic CD spectrum of dCK in

Table 1. Provencher-Glöckner secondary structural analysis of human dCK.

Sample	α-helix (%)	β-sheet (%)	β-turn (%)	Random (%)
dCK	43	40	12	05
dCK + ATP	32	26	23	20
dCK + dCyd	37	25	14	24
dCK + EDTA	39	23	22	16

The concentrations of ATP and dCyd were 20 μM, and the protein to ligand molar ratio was 0.5:1.0. The concentration of EDTA was 6 mM. Secondary structure was calculated from CD spectra (not shown) obtained as described for the representative results shown in Fig. 3.

Marcel Dekker, Inc.
270 Madison Avenue, New York, New York 10016

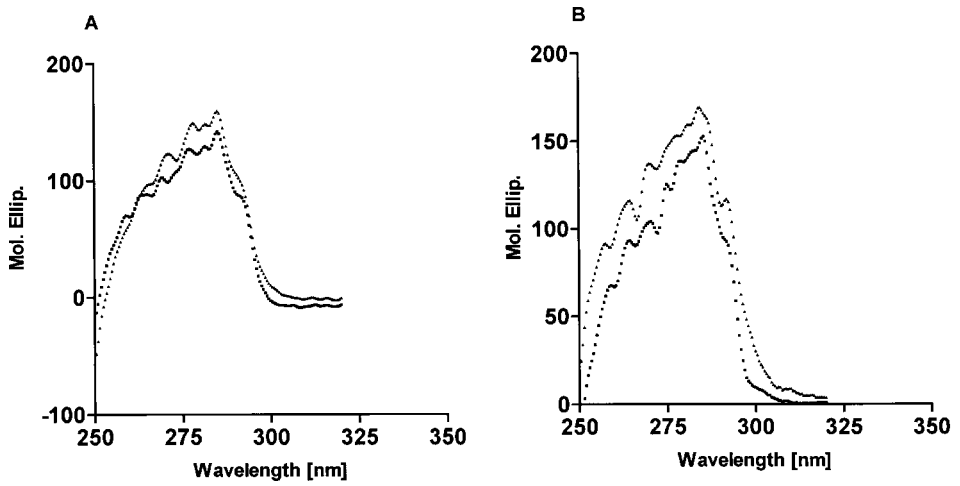

Figure 3. Aromatic CD spectra of human dCK in the absence (■) and presence (▲) of 20 μM UTP (Panel A) and in the absence (■) and presence (▲) of 20 μM gemcitabine (Panel B) in 50 mM potassium phosphate, pH 7.4, 100 mM KCl, 5 mM $MgCl_2$, and 2 mM DTT.

the absence and presence of UTP and gemcitabine, a cytotoxic nucleoside used in solid-tumor chemotherapy, is shown in Fig. 3. The ellipticity of dCK was positive between 255 and 300 nm. The CD band, a shoulder at 291 nm, was due to tryptophan residues, and the bands from 277 to 284 nm and from 260 to 272 nm were due to tyrosine and phenylalanine residues, respectively. Addition of either UTP (Panel A) or gemcitabine (Panel B) perturbed the aromatic residues, resulting in an increase in ellipticity values. Similar, although somewhat smaller, effects were also observed with ATP and dCyd (data not shown).

Analysis of Ligand-Induced Changes in Local Environments of Aromatic Residues in dCK by UV Difference Spectroscopy

The local environments of aromatic residues in a protein can affect its UV absorption spectrum. For example, if the solvent polarity around an aromatic ring decreases as a result of ligand binding, an increase in molar absorptivity (hyperchromic effect) is observed whereas molar absorptivity decreases if the solvent polarity around an aromatic ring increases.[25,26] UV difference spectroscopy was used to assess the effects of ATP, dCyd alone and dCyd in the presence of ATP on the aromatic amino acids of dCK in the experiments of Fig. 4, and Table 2.

Figure 4A shows the difference spectrum of dCK in the presence and absence of ATP. The negative difference peak at 282 nm and the shoulder around 290 nm indicated a blue shift of the tyrosine and trytophan residues, respectively, indicating increased exposure of these aromatic groups to solvent. The number of tryptophan and tyrosine residues perturbed by ATP binding was determined from the observed magnitude of the UV difference spectra in the presence and absence of ATP using the molar absorptivity, ϵ, of tryptophan (5050) and tyrosine (1440). The values of the

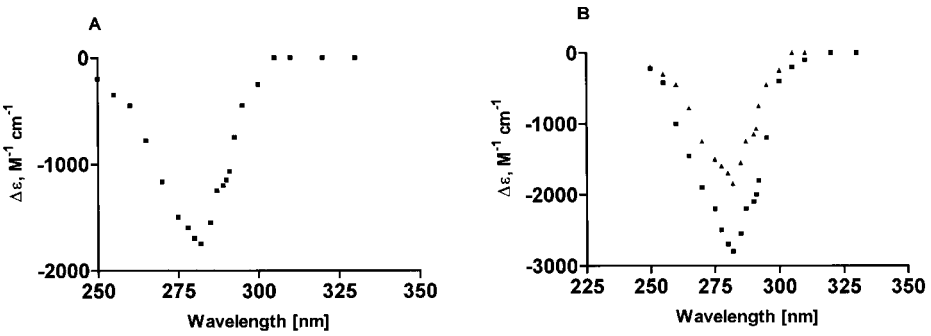

Figure 4. UV difference spectrum of human dCK produced by 10 μM ATP (Panel A) and by 10 μM dCyd (Panel B) in the absence (■) and presence (▲) of ATP. The concentration of dCK used was 16.6 μM in 50 mM potassium phosphate, pH 7.4, 100 mM KCl, 5 mM $MgCl_2$ and 2 mM DTT. The units are expressed as the difference in molar absorption, Δε. After the addition of ATP, the contents of the sample cell were mixed, thereby allowing the interaction to proceed, whereas in the reference cell the protein and the buffer containing ATP were not mixed. Since the concentrations of protein and ATP were identical in both cells, the observed difference in the absorption spectrum was a consequence of their interaction.

molar absorption difference, Δε, at 290 nm (tryptophan) and 282 nm (tyrosine) were 1200 and 1750, respectively, suggesting that one tryptophan and one tyrosine became more exposed to solvent in the presence of ATP.

The effect of binding of the phosphate acceptor, dCyd, to dCK in the absence and presence of the phosphate donor, ATP, on the UV difference spectrum is shown in Fig. 4B. In the absence of ATP, one tryptophan and two tyrosine residues became more exposed to solvent upon binding of dCyd and with Δε values at 290 and 282 nm

Table 2. UV difference spectra of human dCK produced by ligand binding.

Ligand added	Δε, $M^{-1} cm^{-1}$ at 290 nm	Δε, $M^{-1} cm^{-1}$ at 280 nm
ATP	−1100	−1750 (1 tyr)
UTP	−2000	−2750 (2 tyr)
dTTP	−2050	−2750 (2 tyr)
dCTP	−1450	−1900 (1 tyr)
dCyd	−2000	−2850 (2 tyr)
ATP + dCyd	−1100	−1700 (1 tyr)
UTP + dCyd	−1200	−1800 (1 tyr)
gemcitabine	−1850	−3000 (2 tyr)
ATP + gemcitabine	−1700	−1900 (1 tyr)
UTP + gemcitabine	−1200	−1600 (1 tyr)

UV difference spectra were generated with the ligands indicated as described in Fig. 5 and the concentration of ligand used was 10 μM. The magnitude of the change in molar absorptivity was computed from the observed change in absorption for the given protein concentration used. The numbers inside the brackets indicate the number of tyrosine groups affected by the ligand.

Marcel Dekker, Inc.
270 Madison Avenue, New York, New York 10016

of 2100 and 2800, respectively. In the presence of ATP, one tryptophan and one tyrosine residue became more exposed to solvent and with $\Delta\epsilon$ values at 290 and 282 nm of 1150 and 1700, respectively. These results demonstrated that the structure of the ternary complex between dCK, dCyd and ATP differed from that of the binary complexes between dCK and dCyd or dCK and ATP.

The effects of other ligands on dCK are also indicated in Table 2. The difference spectra generated in the presence of UTP or dTTP exposed one tryptophan and two tyrosine residues, whereas the spectra generated in the presence of ATP exposed one tryptophan and one tyrosine residue. The magnitude of exposure of the single tryptophan was greater in the presence of UTP or dTTP than ATP. dCTP, which acts as a feedback inhibitor, behaved like ATP. These results indicated that dCK assumed different conformational states in the presence of the various phosphate donors. Gemcitabine, which behaved like dCyd, exposed one tryptophan and two tyrosine residues when present alone and exhibited the capacity to bind to dCK in the presence of UTP or ATP.

The Effects of ATP and dCyd on Fluorescence of Human dCK

Fluorescence spectroscopy was employed to determine if ATP and dCyd bind to dCK at the same or different sites. Human dCK has 7 tryptophans and 12 tyrosines per monomer which contribute to enzyme fluorescence. When dCK was excited at 285 nm, where both tyrosine and tryptophan residues absorb, its emission maximum was centered at 335 ± 1 nm, indicating that the tryptophans of dCK were partly buried in a nonpolar environment since fully exposed tryptophan residues have an emission maximum at 350 nm. Preliminary studies showed that the fluorescence emission intensity of dCK was quenched by increasing concentrations of either ATP or dCyd, reaching approximately 85% of maximum quenching at 40 μM, the concentration selected for the experiments of Fig. 5. Addition of 40 μM ATP quenched fluorescence

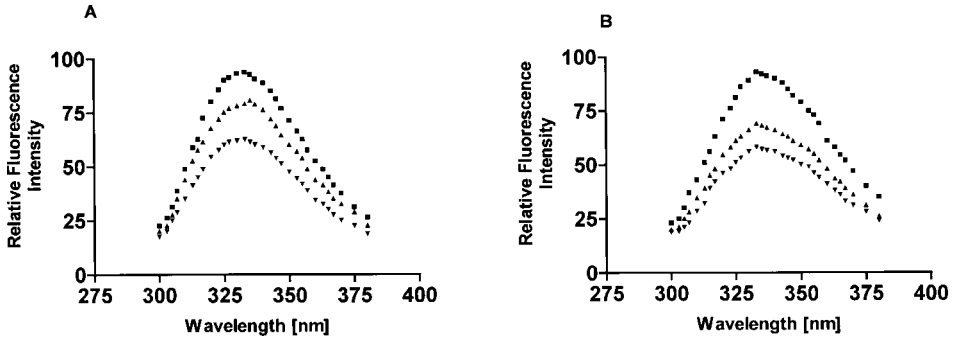

Figure 5. Panel A, fluorescence emission spectra of human dCK alone (■), +40 μM ATP (▲) and +ATP + dCyd (▼). Panel B, dCyd was first added to human dCK, followed by ATP to obtain fluorescence emission spectra of human dCK alone (■), + dCyd (▲), and + dCyd + ATP (▼). The concentration of dCK used was 0.4 μM in 50 mM potassium phosphate, pH 7.4, 100 mM KCl, 5 mM $MgCl_2$ and 2 mM DTT. The excitation wavelength was 285 nm.

MARCEL DEKKER, INC.
270 Madison Avenue, New York, New York 10016

intensity at 335 nm by 12%, and addition of 40 μM dCyd to the dCK-ATP complex caused further quenching, by an additional 23% (Fig. 5A). When dCyd was added first to dCK, fluorescence was quenched by about 27% and the subsequent addition of ATP produced an additional 10% quenching (Fig. 5B). That total quenching was the same in both cases and the order of addition of ligands had no significant effect on the final fluorescence indicated that ATP and dCyd bound to different sites on dCK. These results also indicated formation of ternary complexes between dCK, dCyd and ATP, as suggested in earlier studies.[14,15]

Binding of ATP to dCK was studied in detail by carrying out a fluorescence titration. Addition of ATP resulted in quenching of dCK fluorescence with no change in the emission maximum. A plot of the relative fluorescence intensity vs. the concentration of ATP is shown as an insert in Fig. 6. The maximum quenching in fluorescence intensity observed at saturating concentrations of ATP was taken as 1 and the observed quenching at different concentrations of ATP was plotted as fraction bound vs. ATP concentration (Fig. 6). Nonlinear regression analysis of the binding data revealed unimodal binding with a K_d value of $1.8 \pm 0.4\,\mu M$. The enzyme also bound UTP (data not shown) with high affinity, with a K_d value of $1.9 \pm 0.4\,\mu M$.

The effect of dCyd binding on enzyme fluorescence is shown in Fig. 7. At saturating concentrations of dCyd, the protein fluorescence was quenched by almost 75% (Fig. 7, insert). Nonlinear regression analysis gave a best fit for a two-site (or two-state) model with K_d values of 1.45 ± 0.3 and $150.8 \pm 1.0\,\mu M$, for the high and low

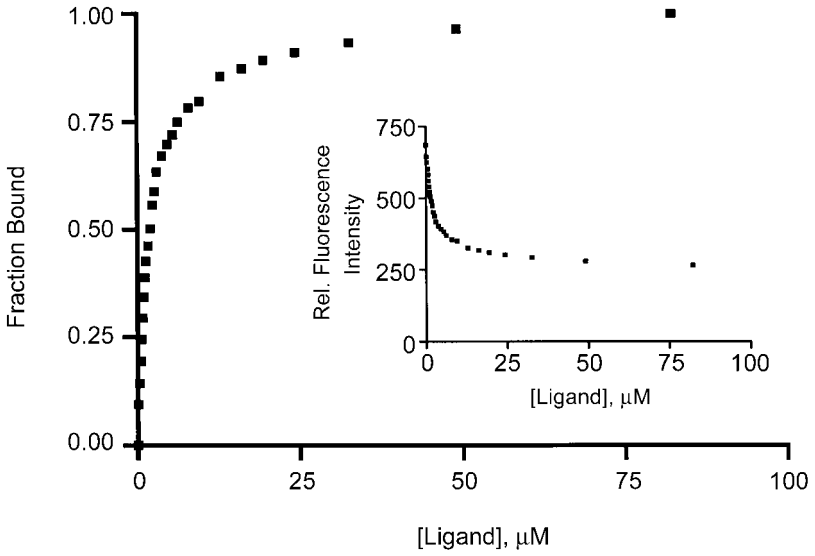

Figure 6. Fluorescence titration of human dCK (0.4 μM) against ATP in 50 mM potassium phosphate, pH 7.4, 100 mM KCl, 5 mM $MgCl_2$ and 2 mM DTT. The protein was excited at 285 nm, and the fluorescence intensity at 335 nm was monitored. Fraction bound vs. ligand concentration is plotted. The insert shows the relative fluorescence intensity at 335 nm as a function of ATP concentration.

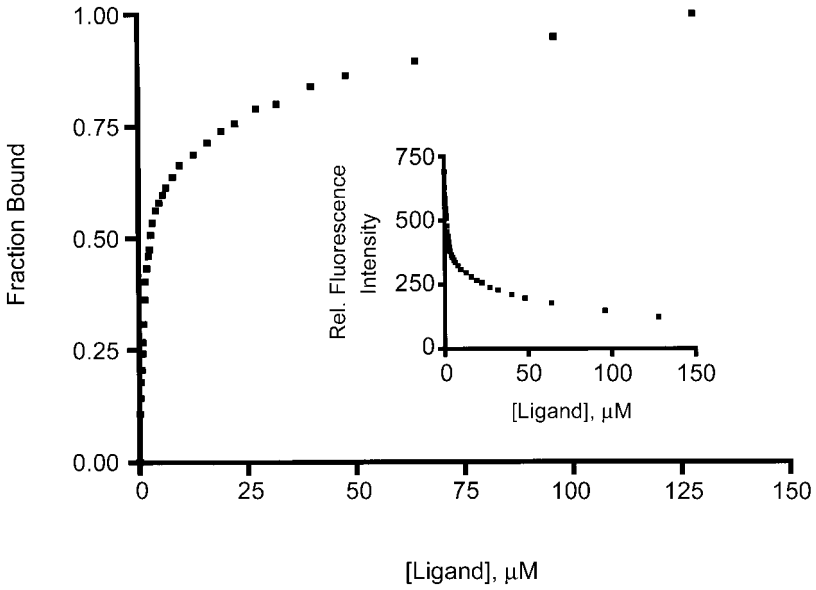

Figure 7. Steady-state quenching of human dCK fluorescence (insert) by dCyd in 50 mM potassium phosphate, pH 7.4, 100 mM KCl, 5 mM $MgCl_2$ and 2 mM DTT. The titration curve is presented as the fraction of dCyd bound as a function of dCyd concentration. The excitation wavelength was 285 nm and the emission intensity was monitored at 335 nm. The protein concentration was 0.4 μM.

affinity sites (or states), respectively. The binding of dCyd to dCK in the presence of 10 μM ATP or UTP (data not shown) also revealed two binding sites, with K_d values of 0.42 ± 0.2 and 40.6 ± 0.3 μM, in the presence of ATP and 1.15 ± 0.2 and 45.5 ± 0.3 μM in the presence of UTP. These findings suggested that the enzyme bound dCyd more tightly in the presence of phosphate donors.

DISCUSSION

The cDNA encoding human dCK has been cloned by Chottiner et al.[3] and the recombinant protein that was produced in *Escherichia coli* had a subunit M_r of 30,500. Human dCK shows 12% sequence similarity with the herpes simplex type 1 virus thymidine kinase (HSV1-TK) and about 40% sequence identity to human mitochondrial thymidine kinase 2 (TK2) and deoxyguanosine kinase (dGK), and these enzymes therefore comprise an enzyme family.[1,4] The crystal structure of dGK with bound ATP was determined recently,[7] and the protein exists as a dimer in the crystals. dCK exhibits significant identity to the sequence of human dGK, and a dimeric model has been proposed for dCK based on the structure of dGK.

The dCK model that is based on the crystal structure of dGK predicts the presence of 6 β-sheets and 7 α-helices with a shallow cleft that comprises the active site.[7] We have confirmed the predicted secondary structure of dCK by CD

measurements. Binding of ATP induced a conformational change in dCK that consisted of a reduction in the α-helical content and an increase in random structure. Addition of dCyd also brought about a change in protein conformation but the magnitude of the change was different and less. These results demonstrated that dCK assumes different conformational states upon binding either ATP or dCyd.

Near-UV CD and UV difference spectroscopy indicated that the binding of ATP to dCK at micromolar concentrations perturbed tryptophan and tyrosine. From the observed magnitude of the UV difference spectra, we estimate that one tryptophan and one tyrosine residue became more exposed to solvent as a consequence of ATP binding. Based on the crystal structure of dGK with bound ATP, we believe these residues in dCK to be tryptophan 58 in helix α2 and tyrosine residue 86 in helix α3. A different result was obtained with the preferred phosphate donor, UTP. The binding of UTP to dCK at micromolar concentrations perturbed three residues, one tryptophan and two tyrosines, demonstrating that dCK assumed different conformational states in the presence of ATP vs. UTP.

The kinetics of phosphorylation of dCyd by dCK are complex and exhibit negative cooperativity with ATP as the phosphate donor, giving Hill coefficients < 1.[11,12] Product inhibition studies have indicated a random bi-bi pathway with ATP, whereas reaction kinetics with UTP followed an ordered A-B random P-Q reaction sequence with UTP as the first substrate to bind.[14] The kinetic data indicate that, although dCK can follow a random bi-bi reaction sequence, the addition of UTP prior to dCyd is preferred when UTP is the phosphate donor. The molecular mechanism of this phenomenon is not clear. Our results demonstrated that dCK assumed different conformational states in the presence of ATP and UTP, which may account for the observed kinetic differences in the mode of phosphorylation of dCyd.

Addition of dCyd to dCK in the absence of a phosphate donor yielded a UV difference spectrum that corresponded to perturbation of one tryptophan and two tyrosine residues. We speculate, based on the dGK model, that the dCK residues involved were tryptophan 58 in helix α2 and tyrosines 86 and 155 in helices α3 and α6, respectively. The conserved tyrosine in position 155 in dCK corresponds to tyrosine 169 in α6 in dGK and the selectivity of dGK for dGuo is due to the presence of Arg 118 at the active site.[7] Arg 118 provides additional hydrogen bonds to the base, thereby stabilizing purine binding. Arg 118 is held tightly in place by Asp 147, which in turn is positioned by hydrogen bonds to Gln 111, Tyr 169 (α6) and Ser 114. For this reason, we believe that Tyr 155 was perturbed upon binding of dCyd.

Addition of dCyd to dCK in the presence of ATP (i.e., formation of the ternary complex) produced a conformational change that affected one tryptophan and one tyrosine residue. Since binding of ATP to dCK would have already exposed tryptophan 58 in helix α2 and tyrosine 86 in helix α3, the subsequent binding of dCyd would be expected to give a smaller change. In the presence of ATP, tyrosine 86 would move to a more polar environment and the subsequent addition of dCyd would be expected to perturb tyrosine 155 in helix α6. We have also demonstrated the formation of a ternary complex involving dCK, dCyd, and UTP. Another phosphate acceptor, gemcitabine was also shown to form a ternary complex involving dCK and ATP or UTP.

Marcel Dekker, Inc.
270 Madison Avenue, New York, New York 10016

Conformational changes in proteins play an important role in the catalytic mechanisms of many enzymes,[27] including nucleoside monophosphate kinases,[28] phosphoglycerate kinases[29,30] and GTP-binding protein kinases,[31,32] all of which exhibit pronounced domain movements upon nucleotide binding. The results from UV-difference spectroscopy can help to understand the kinetics of phosphorylation of dCyd with either ATP or UTP. Upon binding of either phosphate donor (ATP or UTP) or deoxynucleoside substrates (dCyd or gemcitabine), dCK underwent a conformational change that resulted in the exposure of tyrosine and tryptophan residues at the active site—i.e., the enzyme probably assumed a more open configuration that enabled ATP (or UTP) and dCyd (or gemcitabine) to form a ternary complex leading to catalysis. Since phosphate donors and deoxynucleoside substrates can bind independently and induce a conformational change resulting in the exposure of aromatic residues (Tyr and Trp), the bisubstrate analogue dCTP is able to compete with both ATP and deoxynucleoside substrates.[33] This type of competitive inhibition vs. both substrates is only possible when the reaction mechanism is random and the competing inhibitor can bind to both substrate sites. Our results strongly argue for a random bi-bi mechanism of the reaction catalysed by dCK.

Fluorescence spectroscopy is a powerful technique, not only to look at changes in protein conformation upon ligand binding, but also to determine binding affinities and stoichiometries. By carrying out fluorescence titrations, we found that binding of ATP to dCK was monophasic, with a K_d value of 1.85 μM. By monitoring quenching of the intrinsic fluorescence of recombinant dCK under steady-state conditions, Shafiee et al.[34] also obtained a monophasic binding curve for ATP, with a K_d value of 8.4 μM. Using stopped-flow fluorescence spectroscopy, Turk et al.[15] obtained a K_d value of 22 μM for ATP binding to recombinant dCK. These K_d values were obtained for recombinant dCK that contained the His-tag, whereas our studies were carried out with the recombinant dCK without the His-tag but contained three additional N-terminal amino acids, which may account for the observed higher affinity for ATP.

In summary, we have established that recombinant human dCK exists as a dimer in solution. Binding of ATP had no significant effect on the sedimentation characteristics of dCK under reducing or non-reducing conditions, suggesting that dCK did not aggregate in the presence of ATP. Spectroscopic studies indicated changes in the secondary and tertiary structures of dCK upon ligand binding and the nature and the extent of these changes varied with the ligand and may account for the observed differences in kinetic mechanisms of phosphorylation and substrate specificities.

ACKNOWLEDGMENTS

We thank Robert Luty for CD analysis and Leslie D. Hicks for performing analytical ultracentrifugation experiments. This research was supported by grants from the National Cancer Institute of Canada to CEC and from the Swedish Research Council to SE and by the Alberta Cancer Board and the Faculty of Medicine & Dentistry of the University of Alberta. CEC is Canada Research Chair in Oncology.

REFERENCES

1. Eriksson, S.; Wang, L. Substrate specificity, expression, and primary sequences of deoxynucleoside kinases, implications for chemotherapy. Nucleosides Nucleotides **1997**, *16*, 653–659.
2. Usova, E.V.; Eriksson, S. The effects of high salt concentrations on the regulation of the substrate specificity of human recombinant deoxycytidine kinase. Eur. J. Biochem. **1997**, *248*, 762–766.
3. Chottiner, E.G.; Shewach, D.S.; Datta, N.S.; Ashcraft, E.; Gribbin, D.; Ginsburg, D.; Fox, I.H.; Mitchell, B.S. Cloning and expression of human deoxycytidine kinase cDNA. Proc. Natl. Acad. Sci. USA **1991**, *88*, 1531–1535.
4. Arner, E.S.; Eriksson, S. Mammalian deoxyribonucleoside kinases. Pharmacol. Ther. **1995**, *67*, 155–186.
5. Hengstschlager, M.; Denk, C.; Wawra, E. Cell cycle regulation of deoxycytidine kinase. Evidence for post-transcriptional control. FEBS Lett. **1993**, *321*, 237–240.
6. Johansson, M.; Karlsson, A. Cloning of the cDNA and chromosome localization of the gene for human thymidine kinase 2. J. Biol. Chem. **1997**, *272*, 8454–8458.
7. Johansson, K.; Ramaswamy, S.; Ljungcrantz, C.; Knecht, W.; Piskur, J.; Munch-Petersen, B.; Eriksson, S.; Eklund, H. Structural basis for substrate specificity of cellular deoxyribonucleoside kinases. Nature Structural Biology **2001**, *8*, 616–620.
8. White, J.C.; Capizzi, R.L. A critical role for uridine nucleotides in the regulation of deoxycytidine kinase and the concentration dependence of 1-beta-D-arabinofuranosylcytosine phosphorylation in human leukemia cells. Cancer Res. **1991**, *51*, 2559–2565.
9. Shewach, D.S.; Reynolds, K.K.; Hertel, L. Nucleotide specificity of human deoxycytidine kinase. Mol. Pharmacol. **1992**, *42*, 518–524.
10. Krawiec, K.; Kierdaszuk, B.; Eriksson, S.; Munch-Petersen, B.; Shugar, D. Nucleoside triphosphate donors for nucleoside kinases: donor properties of UTP with human deoxycytidine kinase. Biochem. Biophys. Res. Commun. **1995**, *216*, 42–48.
11. Ives, D.H.; Durham, J.P. Deoxycytidine kinase. 3. Kinetics and allosteric regulation of the calf thymus enzyme. J. Biol. Chem. **1970**, *245*, 2285–2294.
12. Bohman, C.; Eriksson, S. Deoxycytidine kinase from human leukemic spleen: preparation and characteristics of homogeneous enzyme. Biochemistry **1988**, *27*, 4258–4265.
13. Kierdaszuk, B.; Rigler, R.; Eriksson, S. Binding of substrates to human deoxycytidine kinase studied with ligand-dependent quenching of enzyme intrinsic fluorescence. Biochemistry **1993**, *32*, 699–707.
14. Hughes, T.L.; Hahn, T.M.; Reynolds, K.K.; Shewach, D.S. Kinetic analysis of human deoxycytidine kinase with the true phosphate donor uridine triphosphate. Biochemistry **1997**, *36*, 7540–7547.
15. Turk, B.; Awad, R.; Usova, E.V.; Bjork, I.; Eriksson, S. A pre-steady-state kinetic analysis of substrate binding to human recombinant deoxycytidine kinase: a model for nucleoside kinase action. Biochemistry **1999**, *38*, 8555–8561.

Marcel Dekker, Inc.
270 Madison Avenue, New York, New York 10016

16. Babul, J.; Stellwagen, E. Measurement of protein concentration with interferences optics. Anal. Biochem. **1969**, *28*, 216–221.
17. Laue, T.M.; Stafford, W.F. Modern applications of analytical ultracentrifugation. Annu. Rev. Biophys. Biomol. Struct. **1999**, *28*, 75–100.
18. Williams, J.W.; Van Holde, K.E.; Baldwin, R.L.; Fujita, H. The theory of sedimentation analysis. Chem. Rev. **1958**, *58*, 715–806.
19. Laue, T.M.; Shah, B.D.; Ridgeway, T.M.; Pelletier, S.L. In *Analytical Ultracentrifugation in Biochemistry and Polymer Science*, Harding, S.E. Rowe, A.J. Horton, J.C., Eds.; R. Soc. Chem.: Cambridge, U.K. 1991.
20. Mani, R.S.; Karimi-Busheri, F.; Cass, C.E.; Weinfeld, M. Physical Properties of Human Polynucleotide Kinase: Hydrodynamic and Spectroscopic Studies. Biochemistry **2001**, *40*, 12967–12973.
21. Johnson, M.L.; Correia, J.J.; Yphantis, D.A.; Halvorson, H.R. Analysis of data from the analytical ultracentrifuge by nonlinear least-squares techniques. Biophys. J. **1981**, *36*, 575–588.
22. Cohn, E.J.; Edsall, J.T. In *Proteins*, Cohn, E.J. Edsall, J.T., Eds.; Reinhold Publishing Corporation: New York, NY 1943.
23. Mani, R.S.; Kay, C.M. Isolation and characterization of a novel molecular weight 11,000 $Ca_2(+)$-binding protein from smooth muscle. Biochemistry **1990**, *29*, 1398–1404.
24. Provencher, S.W.; Glöckner, J. Estimation of globular protein secondary structure from circular dichroism. Biochemistry **1981**, *20*, 33–37.
25. Donovan, J.W. In *Physical Principles and Techniques of Protein Chemistry*, Leach, S.J., Eds.; Academic Press: New York, NY 1969.
26. Donovan, J.W. Ultraviolet difference spectroscopy–new techniques and applications. Methods Enzymol. **1973**, *27*, 497–525.
27. Gerstein, M.; Lesk, A.M.; Chothia, C. Structural mechanisms for domain movements in proteins. Biochemistry **1994**, *33*, 6739–6749.
28. Muller, C.W.; Schlauderer, G.J.; Reinstein, J.; Schulz, G.E. Adenylate kinase motions during catalysis: an energetic counterweight balancing substrate binding. Structure **1996**, *4*, 147–156.
29. Banks, R.D.; Blake, C.C.; Evans, P.R.; Haser, R.; Rice, D.W.; Hardy, G.W.; Merrett, M.; Phillips, A.W. Sequence, structure and activity of phosphoglycerate kinase: a possible hinge-bending enzyme. Nature **1979**, *279*, 773–777.
30. Watson, H.C.; Walker, N.P.; Shaw, P.J.; Bryant, T.N.; Wendell, P.L.; Fothergill, L.A.; Perkins, R.E.; Conroy, S.C.; Dobson, M.J.; Tuite, M.F.; et al., Sequence and structure of yeast phosphoglycerate kinase. Embo. J. **1982**, *1*, 1635–1640.
31. Pai, E.F.; Krengel, U.; Petsko, G.A.; Goody, R.S.; Kabsch, W.; Wittinghofer, A. Refined crystal structure of the triphosphate conformation of H-ras p21 at 1.35 A resolution: implications for the mechanism of GTP hydrolysis. Embo. J. **1990**, *9*, 2351–2359.
32. Coleman, D.E.; Berghuis, A.M.; Lee, E.; Linder, M.E.; Gilman, A.G.; Sprang, S.R. Structures of active conformations of Gi alpha 1 and the mechanism of GTP hydrolysis. Science **1994**, *265*, 1405–1412.
33. Ikeda, S.; Chakravarty, R.; Ives, D.H. Multisubstrate analogs for deoxynucleoside kinases. Triphosphate end products and synthetic bisubstrate

MARCEL DEKKER, INC.
270 Madison Avenue, New York, New York 10016

analogs exhibit identical modes of binding and are useful probes for distinguishing kinetic mechanisms. J. Biol. Chem. **1986**, *261*, 15,836–15,843.
34. Shafiee, M.; Gosselin, G.; Imbach, J.L.; Eriksson, S.; Maury, G. Synthesis of new fluorescent nucleoside analogues and application to the study of human deoxycytidine kinase. Nucleosides Nucleotides **1999**, *18*, 717–719.

Received July 18, 2002
Accepted December 9, 2002

Marcel Dekker, Inc.
270 Madison Avenue, New York, New York 10016